Comparison of the ligand-binding properties of native and copper-less cytochromes *bo* from *Escherichia coli*

A. John MOODY*, Roy MITCHELL, Alan E. JEAL† and Peter R. RICH†
Glynn Research Foundation, Glynn, Bodmin, Cornwall PL30 4AU, U.K.

The binding of four anionic ligands, cyanide, fluoride, azide and formate, to cytochrome *bo* purified from *Escherichia coli* cells grown with a copper supplement (+Cu cyt.*bo*) is described. Membrane-bound cytochrome *bo* that lacks the copper component, Cu_B, of its active site can be prepared from cells grown under conditions where the availability of copper is limited by the presence of a Cu^I chelator, 2,2′-bicinchinonic acid. The ligand-binding properties of this copper-less enzyme (−Cu cyt.*bo*) are compared with those of +Cu cyt.*bo*. As judged from near-UV/visible spectroscopic changes, cyanide forms a low-spin complex with +Cu cyt.*bo*, whereas azide, fluoride and formate form high-spin complexes. The pH-dependences of binding suggest that for all four of these anionic ligands, both the rates of binding and the binding affinities are primarily dependent on the concentration of their protonated forms. −Cu cyt.*bo*, which shows less than 15 % of the duroquinol oxidase activity of +Cu cyt.*bo*, binds cyanide, azide and fluoride, but with greatly decreased affinity (< 1/30, 1/2000 and 1/2500 respectively at pH 5.5 compared with +Cu cyt.*bo*). The complex of azide with −Cu cyt.*bo* still seems to be high-spin and azide binding to −Cu cyt.*bo* is still pH-dependent, although less so than azide binding to +Cu cyt.*bo*.

INTRODUCTION

Cytochrome *bo* from *Escherichia coli* is a quinol oxidase. Like other members of the haem/Cu terminal oxidase superfamily, it catalyses the reduction of dioxygen to water and couples this highly exergonic reaction to proton translocation across the membrane in which it is embedded [1]. The site of oxygen binding and reduction is a binuclear centre consisting of a type O haem, haem *o*, and a copper, Cu_B. A second haem, haem *b*, might be involved in electron transfer from the quinol substrate to the binuclear centre. *E. coli* cytochrome *bo* does not contain the binuclear copper site, Cu_A, that forms the initial electron acceptor in cytochrome *c* oxidases [2–5].

For bovine cytochrome *c* oxidase we have found that reactions of the binuclear centre involving the uptake of negative charge (either reduction or anion binding) invariably require the uptake of protons [6,7]. This led to the proposal that charge compensation by protonation was a general requirement in the reactions of the haem/Cu oxidases [8], and to a discussion of possible protonmotive mechanisms based on electrostatic principles [9–11]. These notions prompted us to extend our measurements to *E. coli* cytochrome *bo* to probe further the electroneutrality requirement of binuclear centre reactions and to begin to identify both the protonation sites and the access route or routes of protons to these sites. One approach to the latter is to study site-directed mutants chosen with the aid of the accumulated structural knowledge of these enzymes that now includes high-resolution X-ray crystallographic information [3–5]. In this paper, however, we take advantage of the finding that wild-type cytochrome *bo* can assemble without Cu_B when *E. coli* is grown under copper-limited conditions [12–15]. We report the results of an investigation into the ligand-binding properties of the normal copper-containing enzyme and compare them with those of the copper-less enzyme.

EXPERIMENTAL

Spectroscopy and laser-flash photolysis

Optical measurements were made, essentially as described before [16], on single-beam spectrophotometers assembled in-house, except that many of the measurements were made on an instrument constructed around a TM300 monochromator (Bentham Instruments Limited, Reading, Berks., U.K.) in which the gratings are mounted on a rotating turret driven by a microstepping motor. Laser-flash photolysis was performed with a frequency-doubled Nd-YAG laser (Spectron Ltd., Rugby, Warwickshire, U.K.) as described before [15].

Bacterial growth and preparation of membranes

E. coli strain RG145 was used throughout. This strain lacks cytochrome *bd* and overproduces cytochrome *bo* by approx. 5-fold [17]. The growth conditions used were essentially as described before [18], and in all cases growth was continued until stationary phase. When a limit on the availability of copper during growth was required the normal copper supplement (10 μM $CuSO_4$) was omitted and the growth medium was treated with 1 mM ascorbate and 1–2 μM 2,2′-bicinchinonic acid (4,4′-dicarboxy-2,2′-biquinoline, a Cu^I chelator [19,20]), for 1 h at 35 °C before autoclaving. Bacterial membranes were prepared as described before [18].

Abbreviations used: +Cu membranes, those isolated from *E. coli* cells grown with a copper supplement; +Cu cyt.*bo*, cytochrome *bo* with the copper component, Cu_B, of its active site present; −Cu membranes, those isolated from *E. coli* cells grown without a copper supplement and with a copper chelator present; −Cu cyt.*bo*, cytochrome *bo* lacking Cu_B; k_{obs}, observed first-order rate constant for binding; k_{on}, second-order rate constant for binding; k_{off}, first-order rate constant for debinding.

* To whom correspondence should be addressed. Present address: Department of Biological Sciences, University of Plymouth, Drake Circus, Plymouth, Devon PL4 8AA, U.K.
† Present address: Glynn Laboratory of Bioenergetics, Department of Biology, University College, Gower Street, London WC1E 6BT, U.K.

Table 1 The level of copper deficiency of cytochrome *bo* in preparations of membranes from *E. coli* RG145

Preparation of membranes	Measurements (±S.E.M., $n = 3$ throughout) B/A cyanide binding/reduced minus oxidized, $[(\Delta A_{528-548} + \Delta A_{560-576}) \times 0.5]/\Delta A_{560-580(redox)}$	C/A CO binding/reduced minus oxidized, $[(\Delta A_{536-556} + \Delta A_{570-590}) \times 0.5]/\Delta A_{560-580(redox)}$	Ratio (±S.E.M.) (B/A)/(C/A) → B/C	Fraction of +Cu cyt.*bo* (±S.E.M.) relative to preparation 1	Fraction of maximal duroquinol oxidase activity (±S.E.M.) relative to preparation 1
1 (+Cu)	0.183 ± 0.002	0.262 ± 0.001	0.695 ± 0.007	1	1
2 (+Cu)	0.225 ± 0.004	0.315 ± 0.002	0.714 ± 0.003	1.027 ± 0.012	–
3 (−Cu)	0.097 ± 0.001	0.275 ± 0.003	0.352 ± 0.005	0.506 ± 0.009	0.496 ± 0.028
4 (−Cu)	0.082 ± 0.003	0.298 ± 0.006	0.275 ± 0.012	0.393 ± 0.018	–

Measurement of the cytochrome *bo* content of *E. coli* membranes

The CO-binding spectra of fully reduced membranes, which are identical for −Cu and +Cu membranes (isolated from *E. coli* cells grown respectively without a copper supplement and with a copper chelator present, and with a copper supplement) [15], were used to determine the relative cytochrome *bo* content; either $(\Delta A_{536-556} + \Delta A_{570-590}) \times 0.5$ or $\Delta A_{416-430}$ was used, for which the absorption coefficients were taken to be 7 and 196 $mM^{-1} \cdot cm^{-1}$ respectively [15]. Routinely, however, after ligand binding the sample was reduced (for 1 min with 10 mM dithionite), and a dithionite-reduced minus air-oxidized (redox) spectrum generated. For a given membrane preparation there is a reasonably constant relationship between the CO-binding and redox spectra (Table 1). Hence the concentration of enzyme present in individual binding experiments could be determined.

Ligand-binding measurements with membrane-bound cytochrome *bo*

Ligand-binding spectra were obtained as follows. Membranes were diluted in buffer (for pH ⩽ 6.5, 50 mM potassium Mes containing 0.5 mM potassium EDTA; for pH > 6.5, 50 mM potassium phosphate containing 0.5 mM potassium EDTA) to give a concentration of cytochrome *bo* of 1–2 μM, and a baseline scan was taken. The ligand was then added and a scan taken after a set period (5 min with cyanide; 30 s with fluoride and azide). Finally, sodium dithionite (10 mM) was added and a further scan taken after 1 min.

The ligand-binding spectra of cytochrome *bo* lacking Cu_B (−Cu cyt.*bo*) were obtained by subtracting the contribution by cytochrome *bo* with the copper component, Cu_B, of its active site present (+Cu cyt.*bo*) from spectra obtained with membranes isolated from cells grown under copper-limited conditions (−Cu membranes). The contribution by +Cu cyt.*bo* was obtained by appropriate scaling of spectra obtained from +Cu membranes by using both the relative cytochrome *bo* content (see above) and the level of copper deficiency of the cytochrome *bo* in the −Cu membranes (see the Results section).

Measurement of the duroquinol oxidase activity of *E. coli* membranes

The oxidation of duroquinol by *E. coli* membranes at 22–23 °C was monitored by using $\Delta A_{270-285}$. The absorption coefficient for this wavelength pair was taken to be 19.4 $mM^{-1} \cdot cm^{-1}$ [21]. Stock membranes were diluted to give 20–60 nM cytochrome *bo* in 50 mM potassium phosphate, pH 7.5, containing 0.1 mM potassium EDTA. The reaction was started by adding the quinol (as a 20 mM stock in DMSO containing 10 mM HCl).

Preparation of purified +Cu cytochrome *bo*

Cytochrome *bo* was purified as described by Moody and Rich [18]. To ensure that we had a preparation that was both fully oxidized and in the fast form the purified enzyme was 'pulsed' [18,22].

Ligand-binding measurements with purified cytochrome *bo*

The ligand-binding experiments with purified enzyme were performed as follows. A baseline scan with buffer was taken. The buffer was either 50 mM potassium phosphate (pH ⩾ 6.5) or 50 mM potassium Mes (pH ⩽ 6.5), each containing 0.5 mM potassium EDTA. Purified enzyme (fast form) was diluted to 1.5–2 μM in the buffer and a scan taken. The ligand was then added and the time course of binding monitored with appropriate wavelength pairs (e.g. 396/411 nm for fluoride, 412/400 nm and 654/622 nm for azide, and 646/616 nm for formate) after which a final scan was taken.

Analysis of ligand-binding curves and kinetics

A single binding site on the enzyme for each of the ligands was assumed. For azide binding to purified +Cu cyt.*bo*, where K_d and hence the range of ligand concentrations used is comparable to the enzyme concentration used, K_d is given by:

$$K_d = [E]_t(1 - Y)([L]_t - Y[E]_t)/Y[E]_t \quad (1)$$

where $[E]_t$ is the total enzyme concentration, ligated and unligated; $[L]_t$ is the total ligand concentration, bound and unbound; and Y is the fractional saturation of the binding site, which is given by:

$$Y = [EL]/[E]_t = \Delta\epsilon/\Delta\epsilon_\infty \quad (2)$$

where [EL] is the concentration of ligated enzyme, $\Delta\epsilon$ is the change in absorption coefficient observed at a given ligand concentration and $\Delta\epsilon_\infty$ is the change in absorption coefficient at infinite ligand concentration. Eqn. (1) can be rearranged into standard quadratic form, i.e. $ax^2 + bx + c = 0$, where $a = [E]_t$, $b = -([E]_t + [L]_t + K_d)$ and $c = [L]_t$, which, when solved, gives:

$$\Delta\epsilon = \Delta\epsilon_\infty\{[E]_t + [L]_t + K_d - \sqrt{([E]_t + [L]_t + K_d)^2 - 4[E]_t[L]_t}\}/2[E]_t \quad (3)$$

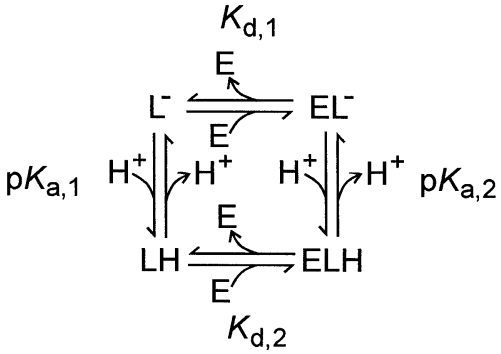

Scheme 1 Model for ligand binding in which the affinity is affected only by the protonation/deprotonation state of the ligand

Eqn. (3) was fitted to the azide-binding curves to obtain values for $\Delta\epsilon_\infty$ and K_d. In all other cases the K_d for the ligand is greatly in excess (more than 40-fold) of the concentration of enzyme used, so eqn. (1) can be reduced to:

$$K_d = [L]_t(1-Y)/Y \quad (4)$$

and rearranged to give:

$$\Delta\epsilon = \Delta\epsilon_\infty[L]_t/(K_d+[L]_t) \quad (5)$$

which was fitted to the ligand-binding curves to obtain values for $\Delta\epsilon_\infty$ and K_d.

The observed first-order rate constants (k_{obs}) for ligand binding were obtained by fitting single-exponential curves to the time courses of binding. Second-order rate constants for binding (k_{on}) were obtained from the slopes of plots of k_{obs} against ligand concentration; first-order rate constants for debinding (k_{off}) were obtained from the *y*-intercepts of the same plots. To obtain more reliable values for the latter, the fits were constrained so that the value for K_d obtained from k_{off}/k_{on} matched that obtained from the binding curves.

Eqn (6) below is derived from the model shown in Scheme 1 on the assumption that the difference between $K_{d,1}$ and $K_{d,2}$ arises solely from the modulation of k_{on} by the protonation/deprotonation of the ligand, i.e. k_{off} is pH-independent:

$$k_{on} = [(k_{on,2}\times 10^{pH-pKa,1})+k_{on,1}]/(1+10^{pH-pKa,1}) \quad (6)$$

When this equation was fitted to plots of k_{on} or k_{obs} (i.e. $k_{on}+k_{off}$) against pH it was clear in all cases that the value of $pK_{a,1}$ obtained was well below the range of pH over which measurements were made. It was assumed that this $pK_{a,1}$ relates to the protonation/deprotonation of the free ligand, and so in subsequent fits its value was constrained to the appropriate pK_a value obtained from the literature.

The curve-fitter embedded in SigmaPlot for Windows 3.1 (Jandel Scientific Software, Erkrath, Germany), which is based on the Marquardt algorithm, was used throughout.

Reagents

All reagents were supplied by Sigma (Poole, Dorset, U.K.) or BDH (Poole, Dorset, U.K.) except the bacterial growth media, which came from Unipath Ltd. (Basingstoke, Hants., U.K.), and Triton X-100 (specially purified for membrane research), which came from Boehringer (Mannheim, Germany). The ligands were all of AnalaR or similar grade. Duroquinol was prepared by reduction of a solution of duroquinone in diethyl ether with aqueous buffered dithionite [23].

RESULTS

Ligand binding to the fast form of oxidized +Cu cyt.*bo*

Although cyanide, fluoride, azide and formate are all known to bind to cytochrome *bo* [22,24–27], few details of the binding processes, e.g. values for k_{on}, k_{off}, K_d and their pH-dependence, have been reported, with the exception of those for azide [28]. We therefore performed a series of such measurements on purified +Cu cyt.*bo* (see Table 2 for a summary).

Binding spectra

Figure 1 shows the difference binding spectra of cyanide (Figure 1A) and of fluoride, azide and formate (Figure 1B). Cyanide induces haem *o* to go low-spin, as indicated by the red shift in the Soret band ($\Delta\epsilon_{420-402}$ 126 $mM^{-1}\cdot cm^{-1}$) and by the disappearance of the charge transfer band at 628 nm ($\Delta\epsilon_{700-628}$ 2.9 $mM^{-1}\cdot cm^{-1}$).

Azide, fluoride and formate all form high-spin complexes with haem *o*, as indicated by the clear retention of the '630 nm' charge transfer band in absolute spectra (results not shown) [26,28], although each is characterized by a new position for the band as shown by the differential features between 600 and 700 nm in the difference spectra shown in Figure 1. From '4th derivatives' [29] of the absolute spectra, λ_{max} for the '630 nm' band is found to be at 619.5, 638 and 645.5 nm for the fluoride, formate and azide complexes respectively. Slight shifts in the position and amplitude of the Soret band are also seen. Fluoride induces a blue shift, whereas azide induces a red shift, and it is noteworthy that the binding spectrum of azide is almost the inverse of that of fluoride over the entire wavelength range examined (390–700 nm). Formate binding is always accompanied by a slight reduction of the low-spin haem *b*, which, although small (less than 5% in the example shown in Figure 1B), badly distorts the binding spectrum in the Soret region. (An approximately 50:50 mixture of haem types B and O [30] is present at the low-spin site of our purified +Cu cyt.*bo*. A similar mixture is seen in membranes derived from cells grown with a copper limitation.) Correction for this distortion (results not shown), by using the redox spectrum for the low-spin site obtained immediately after the addition of dithionite to formate-ligated enzyme, reveals a binding spectrum that is qualitatively similar to that for azide in the range 500–700 nm. A slight blue shift in the Soret absorption band seems to be caused by an increase in the amplitude of the Soret band of haem *o* at 406 nm ($\Delta\epsilon_{406}$ approx. 10–15 $mM^{-1}\cdot cm^{-1}$) rather than by a shift in the $\lambda_{max.}$ of haem *o*.

With fluoride and azide, both the shift in the Soret band and the shift in the charge transfer band are suitable for monitoring the ligand-binding kinetics. The fluoride-binding spectrum is unchanged over the pH range 6.0–8.0, whereas the azide-binding spectrum is unchanged over the pH range 5.5–7.5, but between pH 7.5 and 8.5 $\Delta\epsilon_{412-400}$ decreases by 30–40%. This is caused by a slight pH-dependence of the spectra of both the unligated and the azide-ligated enzyme. A much smaller decrease in $\Delta\epsilon_{654-622}$ is seen (less than 10%), which is caused by a slight pH-dependence of the spectrum of the unligated enzyme. With formate, because of the slight reduction of haem *b*, only the shift in the charge transfer band is suitable. For all three ligands binding is monophasic.

Table 2 Summary of ligand binding to ferric + Cu cyt.*bo*

Principal bound species at pH 6.0	Haem *o* spin state	'630 nm' band position (nm)	Binding kinetics at pH 6.0	Binding parameters		
				k_{on} ($M^{-1} \cdot s^{-1}$)	k_{off} (s^{-1})	K_d (M)
H^+ CN^-	Low	Absent	Monophasic (indications of saturation above 1 mM)	37	Not determined	Not determined
H^+ N_3^-	High	645.5	Monophasic	1.2×10^4	1.4×10^{-2}*	1.2×10^{-6}
H^+ F^-	High	619.5	Monophasic	36	3.1×10^{-3}	8.6×10^{-5}
H^+ HCO_2^-	High	638	Monophasic	2.5	$< 5 \times 10^{-4}$	$< 2 \times 10^{-4}$

* Measured at pH 7.0.

Binding kinetics

Cyanide

Cyanide binding is essentially monophasic with a second-order rate constant of 37 $M^{-1} \cdot s^{-1}$ being found at pH 6.0 with 0.2–1 mM KCN. This rate constant is slightly pH-dependent, increasing by approx. 1.8-fold over the pH range 6.0–8.5 (results not shown).

Fluoride

Figure 2(A) shows plots of the maximal extent of $\Delta\epsilon_{396-411}$ against concentration of fluoride at pH 6.0, 7.0 and 8.0. K_d values (means ± S.E.M.) of 0.086 ± 0.007, 0.84 ± 0.05 and 5.6 ± 0.9 mM at pH 6.0, 7.0 and 8.0 respectively are obtained from a global fit of eqn. (5), which describes binding to a single site on the enzyme (see the Experimental section). Figure 2(B) shows plots of k_{obs} against concentration of fluoride for the same pH values. If the K_d values obtained from the data in Figure 2(A) are used to constrain fits to the plots in Figure 2(B), values for k_{off} of $3.1(\pm 2.4) \times 10^{-3}$, $4.9(\pm 1.2) \times 10^{-3}$ and $5.8(\pm 1.8) \times 10^{-3}$ s^{-1} respectively are obtained. Figure 2(C) shows a plot of k_{on} for fluoride against pH. A reasonable fit to this set of data is obtained if k_{on} is modulated by an acid/base group with a pK_a constrained to 3, i.e. the pK_a for hydrofluoric acid [31]. From the fit in Figure 2(C) (see the Experimental section for details), values of k_{on} for hydrofluoric acid and fluoride of $4.3(\pm 0.8) \times 10^4$ and 0.59 ± 0.25 $M^{-1} \cdot s^{-1}$ respectively are obtained.

Azide

A value of 7.9 ± 0.2 μM for K_d is obtained from plots (results not shown) of the maximal extent of $\Delta\epsilon_{412-400}$ and $\Delta\epsilon_{654-622}$ against concentration of azide at pH 7.0, by fitting with eqn. (3) (see the Experimental section). When this value is used to constrain a fit to a plot of k_{obs} against concentration of azide (results not shown) values for k_{on} and k_{off} of $1.7(\pm 0.1) \times 10^3$ $M^{-1} \cdot s^{-1}$ and $1.4(\pm 0.1) \times 10^{-2}$ s^{-1} respectively are obtained. Similar experiments at pH 8.0 and 8.5 (not shown) establish that k_{off} is little affected by pH [$0.6(\pm 0.1) \times 10^{-2}$ s^{-1} at both pH 8.0 and 8.5]. Figure 3 (upper panel) shows a plot of k_{obs} against pH for 20 μM azide. A good fit to this set of data is obtained for a model in which k_{off} is taken to be pH-independent and constrained to 0.9×10^{-2} s^{-1}, and in which k_{on} is modulated by an acid/base group with a pK_a constrained to 4.72, i.e. the pK_a for hydrazoic acid [32]. From this fit, values of k_{on} for hydrazoic acid and hydrazoate of 2.4×10^5 and 170 $M^{-1} \cdot s^{-1}$ respectively are obtained. Direct measurement of k_{on} at pH 8.5 (results not shown), where less than 0.02 % of the azide is present as hydrazoic acid, gives a value of 131 ± 16 $M^{-1} \cdot s^{-1}$.

At pH 7.5 our data are consistent with the K_d of 1.7×10^{-5} M obtained from equilibrium titrations by Little et al. [28] but much less so with the value of 8×10^{-5} M that they obtained from kinetic measurements.

Formate

Formate binding can be monitored by using $\Delta A_{646-616}$, but it is not possible to obtain reliable values for k_{off} either from plots of k_{obs} against formate concentration (results not shown), or for K_d from plots of fraction ligated against formate concentration (results not shown). Nevertheless at pH 5.5 k_{off} is certainly less than 5×10^{-4} s^{-1}, and hence K_d must be less than 0.1 mM. Like k_{obs} for azide binding, k_{obs} for formate binding varies with pH in a manner consistent with the rate of binding being mainly controlled by the concentration of formic acid; the fit shown in Figure 3 (lower panel) (see the Experimental section for details) is constrained to the pK_a of formic acid (3.77) [33].

Quantification of the copper deficiency of cytochrome *bo* in *E. coli* membranes

E. coli RG145 grown under copper-limited conditions can assemble cytochrome *bo* that lacks Cu_B [12–15]. In the present study, rather than simply omitting copper from the growth medium [15], a more reliable copper limitation was produced by using a Cu^I chelator, 2,2′-bicinchinonic acid [19,20]. The level of deficiency during growth could be monitored with room-temperature laser-flash photolysis of the CO compound of fully reduced cytochrome *bo* in cell samples because, with 1 mM CO, the recombination rate for −Cu cyt.*bo* is about 10-fold faster than for +Cu cyt.*bo* [15]. By using concentrations of the chelator in the range 1–2 μM, deficiencies greater than 70 % are obtained. However, the higher concentrations lead to a substantial decrease in the yield of cytochrome *bo*, and at 10 μM chelator the growth is retarded.

−Cu membranes show similar biphasic CO recombination kinetics to the cells from which they were derived, but further attempts to isolate the −Cu cyt.*bo* led to the appearance of a third kinetic phase that has a kinetic spectrum substantially different from those of the other two phases. We have attributed this component to partial denaturation of the −Cu cyt.*bo* during extraction [14]. Hence the ligand-binding experiments on −Cu cyt.*bo* described here were performed with membranes. Although copper deficiencies in excess of 70 % could be obtained, we chose to use membranes where the deficiency was somewhat less but where the optical properties were comparable to membranes derived from cells grown with a copper supplement (+Cu membranes), i.e. where there was no indication that the yield of

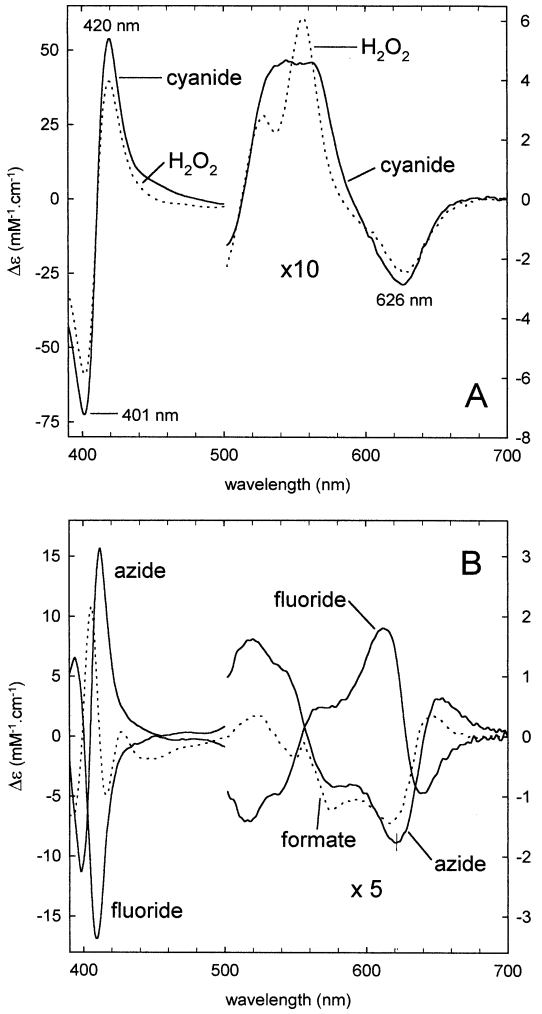

Figure 1 Difference spectra for the binding of (A) cyanide and hydrogen peroxide and (B) azide, fluoride and formate to *E. coli* cytochrome *bo*

A baseline scan with buffer was taken. Purified enzyme (fast form; see the Experimental section) was then diluted to approx. 3.5 μM in the buffer (50 mM potassium phosphate, pH 7.0, containing 0.5 mM potassium EDTA) and a scan taken. Finally the ligand was added and a further scan taken after sufficient time had been allowed for complete binding: 1 min after mixing with 20 mM potassium cyanide; 30 s after mixing with 0.2 mM hydrogen peroxide; immediately after mixing with 2 mM sodium azide; 2 min after mixing with 20 mM sodium fluoride; and 5 min after mixing with 20 mM potassium formate. The concentration of cytochrome *bo* in each case was determined from the A_{406} found before addition of the ligand, using $\epsilon_{406} = 233\ mM^{-1} \cdot cm^{-1}$. In each case the difference spectrum shown is the second spectrum minus the first.

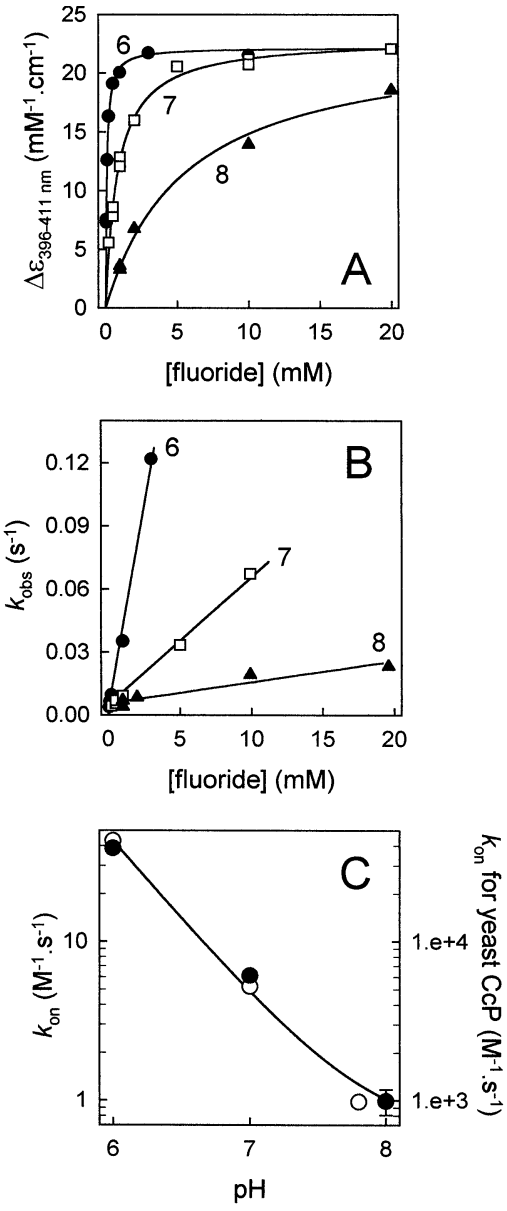

Figure 2 Kinetic plots for the binding of fluoride to *E. coli* cytochrome *bo*

(**A**) Plots of $\Delta\epsilon_{396-411}$ against concentration of sodium fluoride, at p 6.0, 7.0 and 8.0 (as indicated). (**B**) Plots of k_{obs}, derived from time courses of $\Delta\epsilon_{396-411}$, against concentration of sodium fluoride, at pH 6.0, 7.0. and 8.0 (as indicated). (**C**) A plot of $\log_{10}(k_{on})$ against pH with data for yeast cytochrome *c* peroxidase (○, [30]) superimposed for comparison. The curves in each case are fits (see text and the Experimental section).

cytochrome *bo* in the original cells had been depressed by the copper limitation. The relative concentrations of cytochrome *bo* in the various membrane preparations used were obtained from the CO-binding spectra of the fully reduced membranes because CO still binds with high affinity to −Cu cyt.*bo* ($K_d < 7\ \mu$M [10]). The relative proportions of −Cu cyt.*bo* and +Cu cyt.*bo* in a given preparation were obtained from the cyanide-binding spectra of the fully reduced membranes. Because cyanide (at 20 mM) does not bind to fully reduced −Cu cyt.*bo* [10,15], the fraction of binding observed with the −Cu membranes, when compared with that shown by +Cu membranes, was taken as a direct indication of the fraction of +Cu cyt.*bo*. Table 1 shows a summary of the measurements and calculations used to determine both the relative cytochrome *bo* concentrations and the level of copper deficiency of the membrane preparations.

Estimation of the enzyme activity of −Cu cytochrome *bo*

From the relative duroquinol oxidase activities at pH 7.5 and 22–23 °C of −Cu membranes (preparation 3) and +Cu membranes (preparation 1), and the copper deficiency of the −Cu membrane preparation (Table 1), the V_{max} for −Cu cyt.*bo* is estimated to be less than 15% of the V_{max} for +Cu cyt.*bo*. The

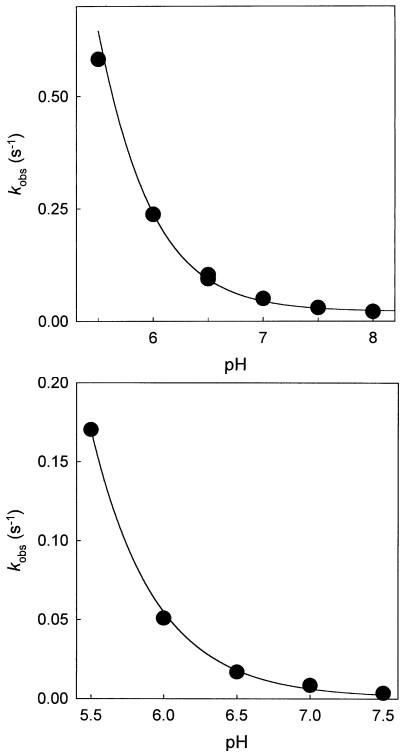

Figure 3 Effect of pH on rates of binding of azide and formate to *E. coli* cytochrome *bo*

Plots of k_{obs} against pH for 20 μM azide (upper panel) and 20 mM formate (lower panel). The curves in each case are fits with eqn. (6) (see text and the Experimental section).

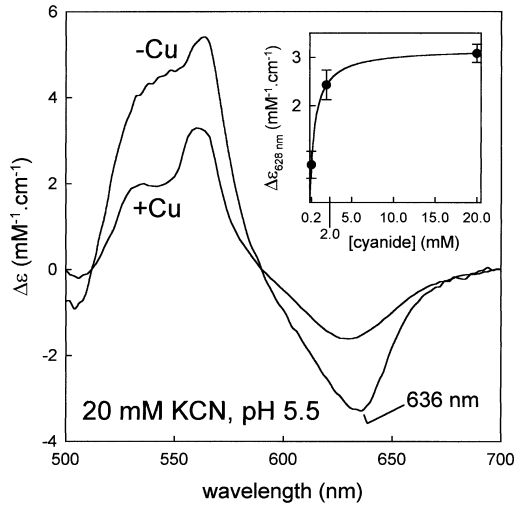

Figure 4 Cyanide binding to copper-less cytochrome *bo*

Binding spectra at 20 mM KCN for −Cu cyt.*bo* and for membrane-bound +Cu cyt.*bo* are shown. These are derived from six measurements each with +Cu and −Cu membranes. A quadratic baseline correction [34], taking 512, 590 and 700 nm as approximate isosbestic points, was used. The inset shows a plot of $\Delta\epsilon_{700-628}$ on cyanide binding to −Cu cyt.*bo* against the concentration of cyanide. The error bars are ± S.E.M. ($n = 6$) and the curve is a best fit with eqn. (5) (see the Experimental section).

apparent K_m for the quinol for +Cu cyt.*bo* and −Cu cyt.*bo* is the same, within experimental error (118 ± 19 μM). The maximal turnover number for +Cu cyt.*bo* with duroquinol as substrate under these conditions is estimated to be 129 ± 15 s^{-1}.

Ligand binding to −Cu cytochrome *bo*

Most of the ligand-binding experiments with −Cu membranes were performed at pH 5.5. This pH was chosen because it represented a practical limit at which the binding of azide, fluoride and formate, i.e. ligands with low pK_a values, could be studied with purified +Cu cyt.*bo* without precipitation problems. For purified +Cu cyt.*bo* the apparent K_d for these ligands decreases as the pH decreases in the range 8–5.5. Hence they are bound most tightly at pH 5.5, making this a good pH to determine whether −Cu cyt.*bo* has a decreased affinity for these ligands.

Cyanide

Figure 4 shows the difference spectrum for cyanide binding to −Cu cyt.*bo*. Qualitatively this spectrum is similar to that of +Cu cyt.*bo* except that the minimum caused by the disappearance of the charge transfer band is red-shifted by approx. 6 nm, to 636 nm. It follows that the charge transfer band itself must be red-shifted by a similar amount in unligated −Cu cyt.*bo*. At −3.3 $mM^{-1}\cdot cm^{-1}$, $\Delta\epsilon_{636}$ is similar to $\Delta\epsilon_{628}$ observed for purified +Cu cyt.*bo* (−2.9 $mM^{-1}\cdot cm^{-1}$). A lower value for $\Delta\epsilon_{628}$, −1.6 $mM^{-1}\cdot cm^{-1}$, is observed on cyanide binding to +Cu cyt.*bo* in membranes (Figure 4).

The inset in Figure 4 shows the $\Delta\epsilon_{700-628}$ for cyanide binding to −Cu cyt.*bo* against the concentration of cyanide, from which a K_d of 0.6 mM is obtained. The $\Delta\epsilon_{700-628}$ values were derived from spectra taken after a 5 min incubation with cyanide. When spectra obtained after a 5 min incubation with 0.2 mM KCN were compared with those obtained after 10 min incubation, no significant difference was found. Hence we can be certain that the binding of cyanide to the −Cu cyt.*bo* was complete within 5 min, and that the data shown in Figure 6 represent a true binding curve.

Fluoride

Figure 5(A) shows difference spectra for fluoride binding to −Cu cyt.*bo*. These spectra are qualitatively similar to the fluoride-binding spectrum of purified +Cu cyt.*bo* shown in Figure 1(B), but the minimum is slightly red-shifted and the difference in absorption coefficient between the maximum and minimum is increased. These differences are consistent with a similar position for the charge transfer band for the fluoride-ligated enzyme irrespective of whether Cu_B is present, and a red-shifted position for the charge transfer band of unligated −Cu cyt.*bo* relative to unligated +Cu cyt.*bo*, for which we already have evidence from cyanide-binding spectra (see the previous section). Figure 5(B) shows a plot of the $\Delta\epsilon_{612-640}$ for fluoride binding to −Cu cyt.*bo* against the concentration of fluoride, from which a K_d of 71 mM is obtained. It is important to note here that the data are internally consistent, i.e. there is no significant difference between the results obtained with the two different −Cu preparations used, or indeed between the results obtained with the two different +Cu preparations. The $\Delta\epsilon_{612-640}$ values were derived from spectra taken after a 30 s incubation with fluoride. When spectra obtained after a 30 s incubation with 20 mM NaF were compared with those obtained after 60 s incubation, no significant difference was found. Hence we can be certain that the binding of fluoride to the −Cu cyt.*bo* was complete within 30 s and that the data shown in Figure 5 represent a true binding curve.

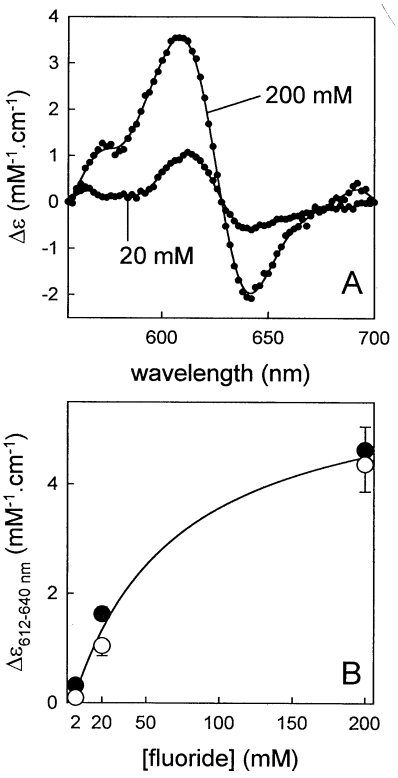

Figure 5 Fluoride binding to copper-less cytochrome *bo*

(**A**) Binding spectra at 20 and 200 mM NaF for −Cu cyt.*bo*. The spectra shown are derived from nine measurements each with +Cu and −Cu membranes for 20 mM NaF, and six measurements each with +Cu and −Cu membranes for 200 mM NaF. A quadratic baseline correction [34], taking 556, 628 and 700 nm as approximate isosbestic points, was used. (**B**) A plot of $\Delta\epsilon_{612-640}$ on the binding of fluoride to −Cu cyt.*bo* against the concentration of fluoride. Data from the two −Cu membrane preparations, which showed no significant differences, were combined. For the open symbols the contribution by +Cu cyt.*bo* was subtracted by using spectra collected for +Cu membrane preparation 1, whereas for the filled symbols the spectra collected for +Cu membrane preparation 2 were used. The error bars are ± S.E.M. and the curve is a best fit with eqn. (5) (see the Experimental section).

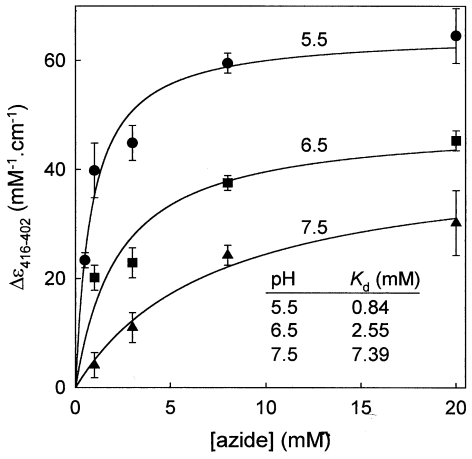

Figure 6 The effect of pH on azide binding to cytochrome *bo* in membranes derived from *E. coli* RG145

The error bars are ± S.E.M. ($n = 4$) in each case. The curves are best fits with eqn. (5) (see the Experimental section).

Azide

The azide-binding spectrum of purified +Cu cyt.*bo* in the range 556–700 nm is dominated by the red-shift in the '630 nm' charge transfer band (Figure 1B), as is the azide-binding spectrum of +Cu membranes, but this feature is essentially absent from the binding spectrum of −Cu cyt.*bo* (results not shown). This difference can be rationalized in the same way as the differences in the fluoride-binding spectra (see above) if the charge transfer band for the azide-ligated enzyme has a similar position whether or not Cu_B is present, and the position for the charge transfer band of unligated −Cu cyt.*bo* is red-shifted relative to unligated +Cu cyt.*bo*. However, in contrast with fluoride, the effect here is to decrease the difference in absorption coefficient between the maximum and minimum. Hence the azide-binding spectrum in the region 556–700 nm is unsuitable for monitoring azide binding, in this case the Soret region is used instead. Figure 6 shows $\Delta\epsilon_{416-402}$ for azide binding to −Cu cyt.*bo* against the concentration of azide, at pH 5.5, 6.5 and 7.5. As with cyanide and fluoride, checks were made to ensure that the time allowed for azide binding (30 s) was sufficient. The inset table in Figure 6 shows the effect of pH in the range 5.5–7.5 on the apparent K_d.

Formate

The presence in *E. coli* RG145 membranes of formate dehydrogenase [35] made it impossible to determine the affinity of the −Cu cyt.*bo* because of continuing reduction of the enzyme by electrons derived from the oxidation of formate.

DISCUSSION

Ligand binding by +Cu cytochrome *bo*

One of the aims of this work was to find out whether the empirical electroneutrality principle that we had established for reactions of the binuclear centre of bovine cytochrome *c* oxidase [6,7] could be applied to another member of the haem/Cu oxidase superfamily, namely *E. coli* cytochrome *bo*. To this end the effect of pH on the binding of four anionic ligands, azide, cyanide, fluoride and formate, to the ferric form of cytochrome *bo* was tested (see Table 2 for a summary of results). Azide and fluoride, which have pK_a values lower than the pH range investigated (5.5–8.0), show pH-dependent binding (i.e. tighter binding at low pH) consistent in both cases with the rate of binding being controlled by the concentration of the protonated form and with net binding of the protonated form (Figures 2C and 3, upper panel). For formate, which also has a low pK_a, the K_d for binding is much lower than the range of formate concentrations tested; furthermore k_{off} is too small to be determined reliably from a plot of k_{obs} against the concentration of formate in this range. Because of the potential difficulty in distinguishing between formate binding/debinding and the interconversion of the fast and slow forms of the enzyme [22], this was not pursued further with lower concentrations of formate. Nevertheless, the pH-dependence of k_{obs} is again consistent with the net binding of the protonated form (Figure 3, lower panel). The k_{on} for cyanide, which has a pK_a value (9.3) [7] higher than the range investigated, shows little dependence on pH; this is also consistent with net binding of the protonated form, but again values for K_d were not determined. Taken together the results indicate that the major effect on the binding of all four ligands relates to the protonation/deprotonation of the ligands

themselves, and that the affinity of the ferric enzyme for the protonated form in each case is several orders of magnitude greater than the affinity for the deprotonated form. In other words, tight binding of these ligands to ferric cytochrome *bo* requires the charge compensation provided by the co-binding of a proton. These results complement the direct measurements that we have made previously with bovine cytochrome *c* oxidase [7], where the binding of the azide, formate, fluoride and cyanide anions was shown to be accompanied by the uptake of a proton. With bovine cytochrome oxidase, however, there are complications that make studying the effect of pH on ligand binding/debinding less useful. For example, formate shows biphasic binding kinetics with bovine cytochrome oxidase [16], and, in addition to reacting with the binuclear centre azide, it can displace one of the axial histidyl ligands of the low-spin haem *a* in this enzyme [36].

For azide and fluoride, where we have more complete information on binding affinity and kinetics, the experimental data were fitted with a simple model in which k_{on} is modulated by protonation/deprotonation of the ligand (see the Experimental section and Scheme 1, where L represents a ligand and E represents the enzyme). Note that k_{off} for both of these ligands is found to be pH-independent within experimental error, and the enzyme seems to have a low but measurable affinity for the deprotonated forms of both ligands. In terms of Scheme 1 we can obtain estimates of $K_{d,1}$ and $K_{d,2}$ by curve-fitting (Figures 2 and 3, upper panel) with $pK_{a,1}$ constrained in each case to the pK_a values for the free ligands (4.72 and 3 for azide and fluoride respectively) [31]. Hence $pK_{a,2}$ for the enzyme–ligand complex can be calculated (approx. 7.9 for both azide and fluoride).

This simple model does not involve any acid/base groups on the unligated enzyme, but despite its success in fitting the data it would be premature to eliminate an involvement of such ionizable groups on the enzyme, because the pH range covered by the data is too restricted. When fitting the data we have assumed the involvement of the protonation/deprotonation of the free ligand and constrained $pK_{a,1}$ accordingly, but these pK_a values are both well below the pH range in which we did our measurements. Free fits to our data are of little use for predicting values for $pK_{a,1}$ and hence are of no use for distinguishing between ligand protonation/deprotonation and enzyme protonation/deprotonation. If we compare fluoride binding to cytochrome *bo* with fluoride binding to yeast cytochrome *c* peroxidase, for which there are data covering the pH range 2.5–9 [32], in both cases over the pH range 6–8 the variation in k_{on} is very similar (Figure 2C) and k_{off} is pH-independent within experimental error. (The values of k_{on} and of k_{off} for cytochrome *c* peroxidase are both about 1000-fold higher than those for cytochrome *bo*. As a result the values of K_d for both enzymes are almost identical in the pH range 6–8.) Nevertheless, for cytochrome *c* peroxidase, from data in the pH range 2.5–5.5, there is clear evidence for the involvement of an acid/base group on the enzyme with a pK_a of approx. 5.5, and confirmatory evidence for this group has come from the pH-dependence, in the same range, of the kinetics of cyanide binding to cytochrome *c* peroxidase [37]. Something similar is certainly possible for *E. coli* cytochrome *bo*, but although further kinetic information, at least for azide, could be obtained by using stopped flow, the major limitation in extending the pH range for any ligand is the increasing instability of the enzyme at extreme pH. It should be noted, however, despite the limitations of the data, that there is a clear contrast between the behaviour of cytochrome *bo* (and also of cytochrome *c* peroxidase) and that of metmyoglobin, for example, where the binding of anionic ligands does not require the co-binding of a proton [38] (for further discussion see [10]).

Table 3 Ligand binding to +Cu cyt.*bo* and −Cu cyt.*bo*

Ligand	Apparent K_d at pH 5.5 (M)	
	+Cu cyt.*bo*	−Cu cyt.*bo*
Cyanide	$< 2 \times 10^{-5}$	6×10^{-4}
Azide	3.5×10^{-7}	7×10^{-4}
Fluoride	2.8×10^{-5}	7×10^{-2}
Formate	$< 1 \times 10^{-4}$	Not determined

Ligand binding by −Cu cytochrome *bo*

The other aim of the work presented here was to determine the effect that the absence of Cu_B has on the binding affinity for the four ligands tested, with a view to assessing the possible contribution of Cu_B to protonation site(s) within the binuclear centre. This was possible for cyanide, azide and fluoride, where reasonable estimates of the binding affinity of −Cu cyt.*bo* were obtained at pH 5.5 (for azide, at pH 6.5 and 7.5 as well), although no attempt was made to measure the binding kinetics other than to establish that binding was complete within the time allowed. With formate, the presence of formate dehydrogenase in the membranes, and the resultant electron flow to cytochrome *bo* from the oxidation of formate, made it impossible to detect binding reliably.

Before discussing the effect of the absence of Cu_B on ligand binding it is worth considering the nature of the copper-less enzyme. Although we can be certain that copper is absent, there is the possibility that it is replaced by another metal. It seems unlikely, however, that it is replaced by paramagnetic nickel or cobalt species because the expected EPR signals are not seen (D. J. B. Hunter, A. J. Moody, P. R. Rich and W. J. Ingledew, unpublished work). Furthermore the CO recombination behaviour of the copper-less enzyme after laser-flash photolysis of the CO compound of the fully reduced enzyme is similar to that shown by two mutant enzymes in which one of the Cu_B ligands, either His-333 or His-334, is replaced with Leu [15,39], and where the metal-binding site is likely to be disrupted [40], which suggests that the copper has not been replaced. The structural integrity of membrane-bound −Cu cyt.*bo* is implied by the similarity of its CO-binding spectrum to that of +Cu cyt.*bo* [15]. This contrasts with the new component that appears on solubilization that we have attributed to denatured −Cu cyt.*bo*, which has a haemoglobin-like CO-binding spectrum where the maxima and minima in the visible region are red-shifted by approx. 10 nm relative to +Cu cyt.*bo* [14]. It is possible that maintenance of the structural integrity of the enzyme in the absence of Cu_B might require charge compensation, e.g. the protonation of one of its histidyl ligands, but this might not be necessary if negative charge, e.g. in the form of missing hydroxy ligands to haem *o*, Cu_B or to both metals, is also absent.

Returning to the question of the effect that the absence of Cu_B has on the binding of cyanide, azide and fluoride to cytochrome *bo*, it seems clear that it causes a considerable decrease in the affinity of the enzyme for all three ligands (Table 3). Nevertheless potential complications in the use of membranes for binding studies warrant some discussion of the validity of our binding data. With +Cu cyt.*bo*, where the enzyme is active, the principal problem with studying ligand binding is continuing slow turnover of the enzyme in membranes, resulting in a significant level of turnover intermediates such as F• [18] being present. The ligand might not bind to a fraction of the enzyme

and, even if it does, the binding spectrum is likely to be substantially different. The consequences of this can be seen in the cyanide-binding spectrum for +Cu membranes shown in Figure 4: although the spectrum is qualitatively the same as that found with purified +Cu cyt.*bo*, the amplitude is much lower ($\Delta\epsilon_{700-628}$ is only approx. 55% of that in Figure 1A). A similar decrease (to 46%) in the amplitude of $\Delta\epsilon_{654-622}$ is found with azide (results not shown), although again the binding spectrum is qualitatively the same as that found with purified +Cu cyt.*bo*.

With −Cu cyt.*bo*, however, the presence of turnover intermediates seems not to be a problem. The enzyme has little (less than 15% duroquinol oxidase) or possibly no activity, and the available evidence suggests that the form present in our membranes is essentially fully oxidized. The binding spectrum for cyanide shown in Figure 4 has a distinct minimum caused by the loss on binding of the '630 nm' charge transfer band and this minimum has an absorption coefficient that is essentially the same as that found for cyanide binding to purified +Cu cyt.*bo*. This suggests that haem *o* is mostly oxidized; if it were anything other than oxidized we would expect this band to be already absent before binding, and hence cyanide could not induce the appearance of a minimum at this position. It is also probable that haem *b* in the −Cu cyt.*bo* fraction is mostly oxidized before ligand binding because the ratio of $\Delta A_{416-430}$ (CO binding) to $\Delta A_{428-460}$ (redox) that we find is the same within experimental error as that found for purified +Cu cyt.*bo* (0.89 ± 0.07, compared with 0.83 from Table 1 in [15]). There is also no evidence in our spectra (Figures 4 and 5A, and results not shown) for significant reduction of haem *b* concomitant with ligand binding on the time scale of our experiments. Overall, therefore, it seems that our results reliably reflect ligand binding to fully oxidized −Cu cyt.*bo*, and hence comparison with the results obtained with purified fully oxidized +Cu cyt.*bo* is justified.

By analogy with bovine cytochrome oxidase it is conceivable that both cyanide [41] and azide [36,41] might form bridges between the haem iron and Cu_B in cytochrome *bo*. Indeed, Li and Palmer [36] have suggested that the formation of a high-spin complex of the bovine enzyme with azide, rather than the expected low-spin complex, might arise from the modulation of the ligand-field strength of azide through its co-ordination to Cu_B. Hence the decrease in the affinity of cytochrome *bo* for cyanide and azide when Cu_B is absent could be caused by the loss of part of their binding sites. For azide, where Little et al. [28] have argued that the binding site on *E. coli* cytochrome *bo* is Cu_B, this is an even more reasonable explanation. Nevertheless azide still seems to be able to form a complex with cytochrome *bo* when Cu_B is absent, and this complex still seems to be high-spin because there is no minimum in the binding spectrum corresponding to the loss of the '630 nm' charge transfer band (results not shown). This contrasts with the low-spin cyanide complex, where the '630 nm' charge transfer band is clearly lost (Figure 4).

It also seems that fluoride, like cyanide and azide, can bind when Cu_B is absent, but again with much lower affinity. For yeast cytochrome *c* peroxidase it has been suggested that the preferential binding of HF arises from stabilization of the complex by a hydrogen-bonding interaction with the distal histidine (His-52) [42]. From the hydrogen-bonding system in which His-52 is involved in the unligated cytochrome *c* peroxidase, it is presumed that it accepts a hydrogen bond from HF, but if it were protonated on ligand binding then it could act as hydrogen-bond donor to F^- instead [43]. A similar role might be filled by a Cu_B ligand in the net binding of HF to cytochrome *bo*. Hence Cu_B can be seen both as part of the ligand-binding site and as the binding site of a charge-compensating proton.

For azide, where we were able to determine the pH-dependency of K_d over a limited range for both +Cu cyt.*bo* and −Cu cyt.*bo*, K_d is still pH-dependent in the absence of Cu_B, although the stabilization of the ligand–enzyme complex by the co-binding of a proton is less for −Cu cyt.*bo* than for +Cu cyt.*bo*. This suggests that charge compensation can still occur in the absence of Cu_B. It should be noted that although we find with +Cu cyt.*bo* that the kinetically active species of each ligand is the protonated form, this might not be so for −Cu cyt.*bo*. We have recently found that the kinetically active species is CN^- rather than HCN in the binding of cyanide to a mutant form of horseradish peroxidase in which the distal histidine (His-42) is replaced by Leu, whereas in the native enzyme, where cyanide binds much more strongly, the kinetically active species is HCN. Nevertheless in the mutant the net bound species is still HCN (B. Meunier and P. R. Rich,, unpublished work). The implications are that the proton-binding site is more remote from the anion-binding site in the mutant, and that the binding routes of the anion and the proton are now independent. This might also be so for cytochrome *bo* that lacks Cu_B.

REFERENCES

1 Trumpower, B. L. and Gennis, R. B. (1994) Annu. Rev. Biochem. **63**, 675–716
2 Lappalainen, P. and Saraste, M. (1994) Biochim. Biophys. Acta **1187**, 222–225
3 Tsukihara, T., Aoyama, H., Yamashita, E., Tomizaki, T., Yamaguchi, H., Shinzawa-Itoh, K., Nakashima, R., Yaono, R. and Yoshikawa, S. (1995) Science **269**, 1069–1074
4 Iwata, S., Ostermeier, C., Ludwig, B. and Michel, H. (1995) Nature (London) **376**, 660–669
5 Tsukihara, T., Aoyama, H., Yamashita, E., Tomizuki, T., Yamaguchi, H., Shinzama-Itoh, K., Nakashima, R., Yaono, R. and Yoshikawa, S. (1996) Science **272**, 1136–1144
6 Mitchell, R., Mitchell, P. and Rich, P. R. (1992) Biochim. Biophys. Acta **1101**, 188–191
7 Mitchell, R. and Rich, P. R. (1994) Biochim. Biophys. Acta **1186**, 19–26
8 Rich, P. R., Brown, S., Moody, A. J. and Mitchell, J. R. (1993) Biol. Chem. Hoppe-Seyler **374**, 823
9 Rich, P. R. (1995) Aust. J. Plant Physiol. **22**, 479–486
10 Rich, P. R., Meunier, B., Mitchell, R. M. and Moody, A. J. (1996) Biochim. Biophys. Acta **1275**, 91–95
11 Rich, P. R. (1996) in Protein Electron Transfer, (Bendall, D. S., ed.), pp. 217–248, BIOS Scientific Publishers, Oxford
12 Salerno, J. C., Bolgiano, B., Poole, R. K., Gennis, R. B. and Ingledew, W. J. (1990) J. Biol. Chem. **265**, 4364–4368
13 Ciccognani, D. T., Hughes, M. N. and Poole, R. K. (1992) FEMS Microbiol. Lett. **94**, 1–6
14 Moody, A. J., Mitchell, J. R., Brown, S. and Rich, P. R. (1993) Biol. Chem. Hoppe-Seyler **374**, 822
15 Mitchell, R., Moody, A. J. and Rich, P. R. (1995) Biochemistry **34**, 7576–7585
16 Moody, A. J., Cooper, C. E. and Rich, P. R. (1991) Biochim. Biophys. Acta **1059**, 189–207
17 Au, D. C.-T. and Gennis, R. B. (1987) J. Bacteriol. **169**, 3237–3242
18 Moody, A. J. and Rich, P. R. (1994) Eur. J. Biochem. **226**, 731–737
19 Case, D. A. and Karplus, M. (1979) J. Mol. Biol. **132**, 343–368
20 Brenner, A. J. and Harris, E. D. (1995) Anal. Biochem. **226**, 80–84
21 Zweck, A., Bechmann, G. and Weiss, H. (1989) Eur. J. Biochem. **183**, 199–203
22 Moody, A. J., Cooper, C. E., Gennis, R. B., Rumbley, J. N. and Rich, P. R. (1995) Biochemistry **34**, 6838–6846
23 Rich, P. R. (1981) Biochim. Biophys. Acta **637**, 28–33
24 Ingledew, W. J., Horrocks, J. and Salerno, J. C. (1993) Eur. J. Biochem. **212**, 657–664
25 Moody, A. J., Rumbley, J. N., Gennis, R. B., Ingledew, W. J. and Rich, P. R. (1993) Biochim. Biophys. Acta **1141**, 321–329
26 Watmough, N. J., Cheesman, M. R., Gennis, R. B., Greenwood, C. and Thomson, A. J. (1993) FEBS Lett. **319**, 151–154
27 Calhoun, M. W., Gennis, R. B., Ingledew, W. J. and Salerno, J. C. (1994) Biochim. Biophys. Acta **1206**, 143–154
28 Little, R. H., Cheesman, M. R., Thomson, A. J., Greenwood, C. and Watmough, N. J. (1996) Biochemistry **35**, 13780–13787
29 Butler, W. L. (1979) Methods Enzymol. **56**, 501–515
30 Puustinen, A., Morgan, J. E., Verkhovsky, M., Thomas, J. W., Gennis, R. B. and Wikström, M. (1992) Biochemistry **31**, 10363–10369

31 Dawson, R. M. C., Elliott, D. C., Elliott, W. H. and Jones, K. M. (1986) Data for Biochemical Research. Oxford Science Publications, Oxford
32 Erman, J. E. (1974) Biochemistry **13**, 34–39
33 Allinger, N. L., Cava, M. P., De Jongh, D. C., Johnson, C. R., Lebel, N. A. and Stevens, C. L. (1971) Organic Chemistry, Worth Publishers, New York
34 Brown, S., Colson, A.-M., Meunier, B. and Rich, P. R. (1993) Eur. J. Biochem. **213**, 137–145
35 Prebble, J. N. (1981) Mitochondria, Chloroplasts and Bacterial Membranes, Longman, New York
36 Li, W. and Palmer, G. (1993) Biochemistry **32**, 1833–1843
37 Erman, J. E. (1974) Biochemistry **13**, 39–44
38 Brancaccio, A., Cutruzzolà, F., Allocatelli, C. T., Brunori, M., Smerdon, S. J., Wilkinson, A. J., Dou, Y., Keenan, D., Ikeda-Saito, M., Brantley, R. E. J. and Olson, J. S. (1994) J. Biol. Chem. **269**, 13843–13853
39 Brown, S., Rumbley, J. N., Moody, A. J., Thomas, J. W., Gennis, R. B. and Rich, P. R. (1994) Biochim. Biophys. Acta **1183**, 521–532
40 Minagawa, J., Mogi, T., Gennis, R. B. and Anraku, Y. (1992) J. Biol. Chem. **267**, 2096–2104
41 Thomson, A. J., Greenwood, C., Gadsby, P. M. A., Peterson, J., Eglinton, D. G., Hill, B. C. and Nicholls, P. (1985) J. Inorg. Biochem. **23**, 187–197
42 Edwards, S. L., Poulos, T. L. and Kraut, J. (1984) J. Biol. Chem. **259**, 12984–12988
43 Edwards, S. L. and Poulos, T. L. (1990) J. Biol. Chem. **265**, 2588–2595

Received 22 November 1996/10 February 1997; accepted 20 February 1997